Forced Rayleigh Scattering

D. W. Pohl, S. E. Schwarz,* and V. Irniger
IBM Zurich Research Laboratory, 8803 Rüschlikon, Switzerland
(Received 9 April 1973)

A sensitive Rayleigh-scattering technique has been developed which combines the advantages of stimulated and classical scattering. Forward Rayleigh scattering (3-mrad angular separation) in NaF was observed between 300 and 20°K. The scattered intensity varies by more than 4 orders of magnitude within this temperature interval. Quantitative agreement with theoretical values based on the Landau-Placzek theory is found for $T > 80$°K. Scattering rates considerably larger than expected are found for lower temperatures.

Light scattering is a powerful tool for the investigation of thermodynamic fluctuations in transparent materials. In spite of its large sensitivity, however, there remain interesting interactions which are still below the level of detectability. Particular difficulties are encountered with scattering in the forward direction and at the "central" peak because of superposed stray light. At low temperatures the detection of the central or Rayleigh peak is further obstructed by very weak coupling between entropy (temperature) fluctuations and light.[1,2] The few published data on Rayleigh scattering in solids reflect this situation. On the other hand, detailed experimental knowledge on the central peak in the scattered spectrum could substantially heighten the insight into such phenomena of current interest as phase transitions and collective modes—for example, second sound in dielectric crystals.

In an attempt to overcome these difficulties we have performed a scattering experiment with an artificial, strong temperature fluctuation generated by means of two intersecting, slightly absorbed laser beams. The resulting thermal grating was intense enough to cause strong scattering (or diffraction) of a probing beam of different wavelength even under the above-mentioned unfavorable conditions; for example, scattered light was clearly detected in NaF at 20°K at an angle of only 3 mrad with respect to the incident beam. The increased sensitivity results from a favorable combination of the features of classical and stimulated scattering which, for distinction, shall be called "forced" Rayleigh scattering.

The theory of forced Rayleigh scattering is readily derived from that of stimulated Rayleigh scattering.[3,4] The amplitude δT and the grating constant $\vec{k}$ are given by the wave vectors $\vec{k}_1$, $\vec{k}_2$ and the intensities I_1, I_2 of the two exciting waves:

$$\vec{k} = \vec{k}_1 - \vec{k}_2, \tag{1}$$

$$\delta T = 2\alpha (I_1 I_2)^{1/2} / k^2 K. \tag{2}$$

The numerator accounts for absorptive (α) heating along the interference structure of the two "pump" light beams [cf. Eqs. (2.11) and (2.11a) of Ref. 4]. The denominator represents the counteraction of heat diffusion with thermal conductivity K. If the pump is modulated with frequency ω the response $\delta T(\omega)$ is reduced by the same Lorentz factor $(1 + 4\omega^2/\Gamma_R^2)^{-1}$ which determines the classical Rayleigh line. Γ_R is the inverse of the transient thermalization time:

$$\tau_R = 2/\Gamma_R = C_p / k^2 K \tag{3}$$

and depends on the volume specific heat C_p. With the parameters of our experiment (see below) we find, for example, $\delta T = 1$ mdeg at 300°K and 0.02 mdeg at 30°K as compared to a statistical fluctuation[5] $\langle \Delta T^2 \rangle^{1/2} = 0.6 \times 10^{-9}$ and 0.4×10^{-9} deg, respectively.

The relation between the amplitudes and wave vectors of the incident $(E_3, \vec{k}_3)$ and the scattered $(E_4, \vec{k}_4)$ radiation is derived either also from the theory of stimulated scattering[3,4] or, alternatively, from that of dielectric volume gratings[6]:

$$(\vec{k}_4 \cdot \nabla) E_4 = i k_4^2 (n^{-1} \partial n / \partial T)_{\text{eff}} \delta T E_3, \tag{4}$$

$$\vec{k}_3 - \vec{k}_4 = \vec{k}. \tag{5}$$

The derivative of the refractive index n has to be taken with the constraints discussed below and, in more detail, by Pohl and Schwarz[2] and Wehner and Klein.[7]

The experimental arrangement is depicted in Fig. 1. As a first application we have chosen the forward Rayleigh scattering in NaF which is of interest for the phenomenon of second sound.[8]

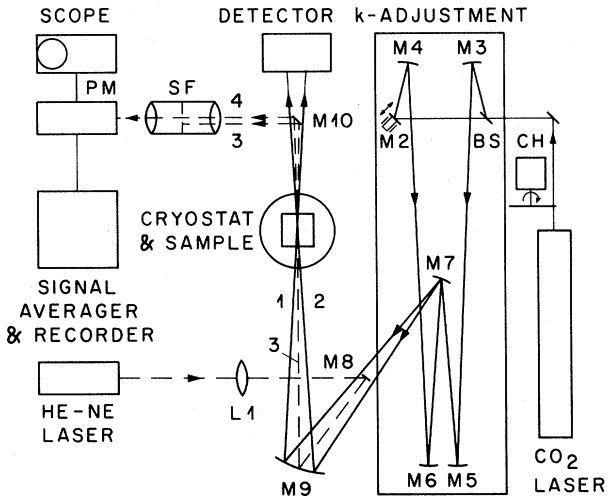

FIG. 1. Experimental arrangement.

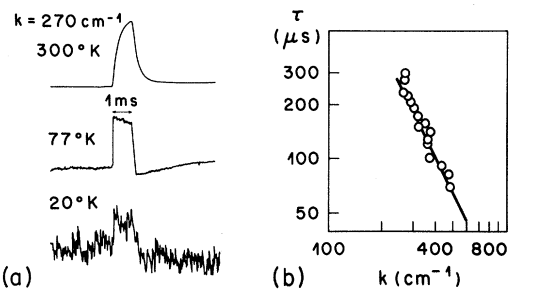

FIG. 2. (a) Scattered signal (averaged over 2^{14} pulses) at three temperatures. (b) Decay time versus grating constant.

The pump light source is a 10-W CO_2 laser, the wavelength of which just falls into the short-wavelength tail of the Reststrahlen band of NaF[9] ($\alpha = 0.3$ to $0.5\ cm^{-1}$ depending on T). The laser beam is sent through a chopper CH, generating pulses of duration $t_p = 0.17$ or 1.0 msec at a repetition rate of 47.3 Hz or multiples of this frequency. Two beams, 1 and 2, of equal intensity are produced by an appropriately coated Ge beam splitter BS. They are sent through the enframed system of mirrors which allows adjustment of spatial frequency, orientation, and (by means of the loudspeaker-mounted mirror M2) phase of the interference pattern at M7. Then the radiation is imaged into the sample by means of mirror M9 which also serves to couple the light of the probe beam 3 from the He-Ne laser into the sample.

The sample, a ⟨100⟩-oriented normal-quality NaF crystal[10] of 2-cm length and 1-cm diameter, is mounted on a cool finger within a Dewar (T = 15–300°K). The laser beams illuminate an area approximately 3 mm in diameter. About 50% of the radiation is absorbed in the crystal. The angle between the two pump beams can be varied between 45 and 80 mrad resulting in a grating constant k between 270 and 480 cm^{-1} and a scattering angle between 3 and 6 mrad for the 16-times-shorter wavelength of the He-Ne laser. A spatial filter SF behind the cryostat selects the direction of the scattered beam 4. The stray light which also passes through the filter is deliberately enhanced by a thin scratch on the crystal surface in order to have a well-defined local oscillator for heterodyne detection. Hence the received signal is proportional to the amplitude of the scattered radiation, not to its intensity. The electronic detection apparatus consists of a photomultiplier PM, an oscilloscope, and different types of signal averagers (boxcar, lockin, or multichannel analyzer).

The response of the scattered signal to a rectangular pump pulse of 1-msec duration is illustrated best by displays of the multichannel analyzer [Fig. 2(a)]. The slow response at room temperature is clearly distinguished from the rectangular shape of the signals at 77 and 20°K. The difference is caused by the strong increase of K at low temperatures.[8] At 20°K the signal is very weak and scarcely overcomes the random noise. The signal was identified in various ways: (i) It is emitted exactly into the expected direction. (ii) It disappears if one of the pump beams is blocked. (iii) It changes phase when the loudspeaker-mounted mirror M2 is moved. (iv) In one experimental run, a chopper wheel with periodic window arrangements was used. The signals measured at 0.06, 0.3, 1.0, and 3 kHz are on a Lorentzian curve with the expected half-width of about 2 kHz ($T = 315$°K, $k = 430\ cm^{-1}$). (v) Most important, the inverse relationship of E_4 and τ_R to k^2 is experimentally confirmed by the angular dependence of the signal. In Fig. 2(b) the room-temperature experimental decay times as determined from the pulse shape are plotted. The excellent agreement with the theoretical curve as obtained from Eq. (3) with $C_p = 3.14\ J/cm^3\ deg$[11] and $K = 0.2\ W/cm\ deg$[12] is noteworthy. Only at the smallest k is a deviation towards too large values of τ observed, which might be caused by the large wavelength with respect to the illuminated cross section. It should be mentioned that the determination of transient times is equivalent to line-shape measurements [Eq. (3)], another crux in classical

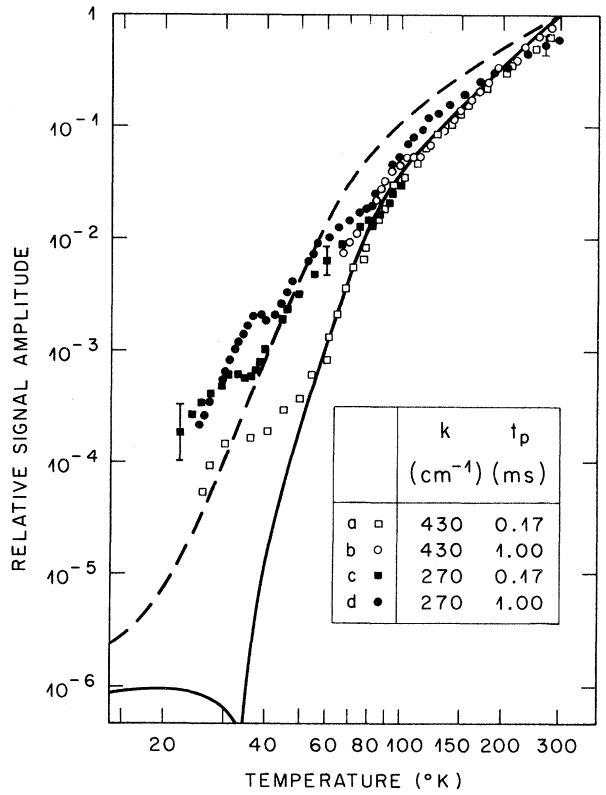

FIG. 3. Signal versus temperature. The symbols refer to different grating constants and pulse widths. The curves refer to theoretical calculations.

scattering due to the frequently very small linewidths.

The temperature dependence of the scattering was investigated quantitatively between 300 and 20°K (Fig. 3). Curves a and d representing the most widely different values of the parameters k and t_p were followed through the whole temperature interval. The other two curves, b and c, were restricted to the high- and low-temperature regions, respectively, for reasons of alignment and because substantial additional information was not expected from a qualitative survey of the omitted regions. The experimental accuracy is limited by the motion of the cool finger (due to thermal expansion) at elevated temperatures and shot noise and output fluctuations of the detection system at low temperatures. The experimental curves are corrected for a temperature-dependent α and normalized to their respective steady-state values at 300°K. The transient times of approximately 300 and 70 μsec at 270 and 430 cm^{-1} (Fig. 2), respectively, then require a reduction of 30% for curves a and d and of 7% for curve b at 300°K.

Two curves calculated from Eqs. (2) and (4) and normalized to 300°K are also shown in Fig. 3. The dashed one is based on the well-known theory of Landau and Placzek which assumes that Rayleigh scattering is caused by purely isobaric temperature fluctuations which couple to a light wave only by thermal expansion. The coupling parameter in Eq. (4) is then simply

$$(n^{-1}\partial n/\partial T)_{\mathrm{eff}} = (n^{-1}\partial n/\partial T)_{\mathrm{LP}} = \beta(\rho n^{-1}\partial n/\partial \rho)_T. \quad (6a)$$

The volume thermal expansion β and $(\rho n^{-1}\partial n/\partial \rho)_T$ (where ρ is the density) have been determined previously.[2] The decrease in scattered amplitude as indicated by the strongly decaying dashed curve is caused by two factors: β is proportional to T^3 at low temperatures, and the heat conductivity may reach a maximum value of about 50 W/cm deg at ~15°K as compared to ~0.2 W/cm deg at room temperature.[12] In the calculation of the solid curve the simplifying assumptions made above were dropped, since temperature fluctuations in solids cannot be completely isobaric and the contribution from direct coupling $(\partial n/\partial T)_\rho$ is not necessarily small.[2,7] The coupling parameter is therefore rewritten

$$\left(\frac{1}{n}\frac{\partial n}{\partial T}\right)_{\mathrm{eff}} = \left(\frac{1}{n}\frac{\partial n}{\partial T}\right)_{\mathrm{LP}}\left[1+\frac{2(\partial n/\partial T)_\rho}{\beta_{\mathrm{eff}} n^3 p_{12}}\right], \quad (6b)$$

with $\beta_{\mathrm{eff}} = \beta(1+2c_{12}/c_{11})/3$, where c_{11}, c_{12}, and p_{12} are the respective elastic and Pockels constants.[2,7] In NaF, the correction tends to reduce the already small low-temperature values obtained above. Even a cancelation due to counteraction of parameters is predicted for $T \simeq 34$°K.[2]

Above approximately 80°K the experimental values agree well with theory, in particular if the signal reduction due to transient effects is corrected for (not shown in Fig. 3). The results presented are, to our knowledge, the first experimental confirmation of the Landau-Placzek theory in solids and with respect to temperature dependence. Moreover, the result emphasizes the relevance of the above-mentioned extension to the original theory.

Below 80°K, experimental results start to deviate in a systematic way from the calculated ones and from each other. The signals are by far too large at low temperatures though the qualitative character of the temperature dependence is preserved. In particular, a flat minimum is observed in each curve at about 30 to 40°K which may be considered as an indication of the pre-

dicted cancelation. During the pulse the crystal temperature rises by one or two degrees which may explain the flatness of the minimum but not the observed absolute magnitude of the signal. Thermalization of the absorbed CO_2-laser radiation might get sufficiently slow at these temperatures to influence the coupling parameter by a nonequilibrium phonon distribution. We do not believe that the investigated normal-quality crystal allows for a well-developed second-sound mode but deviations from the diffusive law might also exist. The answer to these interesting questions will require considerably more work which is beyond the scope of this report. We are planning to extend the forced-Rayleigh-scattering technique to rf-modulated pump radiation in order to investigate the low-temperature Rayleigh peak in more detail.

*Present address: Electrical Engineering Department, University of California, Berkeley, Calif. 94720.

[1]A. Griffin, Rev. Mod. Phys. 40, 167 (1968).

[2]D. W. Pohl and S. E. Schwarz, Phys. Rev. B 7, 2735 (1973).

[3]R. M. Hermann and M. A. Gray, Phys. Rev. Lett. 19, 824 (1967); W. Rother, Z. Naturforsch. 25a, 1120 (1970); H. Eichler, G. Enterlein, J. Munschau, and H. Stahl, Z. Angew. Phys. 31, 1 (1971).

[4]I. P. Batra, R. H. Enns, and D. Pohl, Phys. Status Solidi (b) 48, 11 (1971).

[5]See, for example, L. D. Landau and E. M. Lifshitz, *Statistical Physics* (Pergamon, London, 1958), Sect. 111.

[6]H. Kogelnik, Bell Syst. Tech. J. 48, 2909 (1969).

[7]R. K. Wehner and R. Klein, Physica (Utrecht) 62, 161 (1972).

[8]H. E. Jackson and C. T. Walker, Phys. Rev. B 3, 1428 (1971); S. J. Rogers, *ibid.*, 1440 (1971); the references cited in these two papers.

[9]H. W. Hohls, Ann. Phys. (Leipzig) 29, 433 (1937); D. W. Pohl, to be published.

[10]Supplied by Karl Korth oHG, Kiel, W. Germany.

[11]*Landolt-Börnstein: Zahlenwerte und Funktionen*, edited by K. Schäfer and E. Lax (Springer, Berlin, 1961), 6th ed., Vol. II, Pt. 4, p. 486.

[12]See Jackson and Walker (Ref. 8), Fig. 3, curves *c*, *d*, and *e*. The room-temperature value of K was estimated by extrapolation.

X-Ray Photoemission Study of Some Light Rare-Earth Metals

Y. Baer and G. Busch

Laboratorium für Festkörperphysik, Eidgenössische Technische Hochschule, Hönggerberg, CH-8049 Zürich, Switzerland

(Received 19 April 1973)

We present an x-ray photoemission spectroscopy study of the rare earths La, Ce, Pr, and Nd. We show that the spectra of these metals in the vicinity of the Fermi energy account for the $4f$ levels as well as for the valence states. The energy location of the $4f$ electrons is in fairly good agreement with an existing computation performed in the framework of the renormalized-atom method.

The energy position of the outer electronic levels in rare-earth metals has already been the subject of various photoemission studies.[1-7] Conventional uv light ($\hbar\omega \lesssim 11$ eV) is not very suitable for exciting $4f$ electrons because of the small matrix elements for the excitation of the d states of the continuous spectrum (ϵd) and because of the poor overlap of the $4f$ wave functions with the ϵg wave functions which are hindered by centrifugal repulsion from penetrating deep into the atom cores at low kinetic energies. uv-photoemission spectra give information about valence states but hardly reveal the existence of $4f$ electrons. In contrast, it has been thought until now that soft x-rays would predominantly excite the $4f$ electrons. The spectra of rare-earth metals obtained by x-ray photoemission spectroscopy (XPS) were interpreted exclusively in terms of $4f$ levels and a satisfactory agreement was found with the general predicted features of these states.[1-3] For Sm and Nd, however, the appearance of a peak near the Fermi level does not correspond at all to the expected behavior of the $4f$ electrons as a function of the atomic number. The origin of this peak is not well understood. For example, excited final states are likely to be observed in incomplete shells but they always appear in the spectra at higher binding energies than the ground state. The possible location of the $4f$ ground state just